Exploring liquid–liquid interfaces with transient evanescent grating techniques

Pierre Brodard and Eric Vauthey[a)]
Department of Physical Chemistry of the University of Geneva, 30 Quai Ernest Ansermet, CH-1211 Genève 4, Switzerland

(Presented on 26 June 2002)

A transient grating setup with evanescent wave probing has been developed to investigate ultrafast processes at liquid–liquid interfaces. In order to evaluate the selectivity of this method to the interface, the speed of sound in the low refractive index medium has been measured as a function of the penetration depth of the probe pulse. Our preliminary results indicate an increase of the speed of sound in methanol with decreasing the probe depth from 100 to 70 nm. However, no correlation was found in acetonitrile in the same range. Modifications of the experiment for improving the selectivity to the interface are proposed. © *2003 American Institute of Physics.*
[DOI: 10.1063/1.1517736]

I. INTRODUCTION

Liquid–liquid interfaces play a major role in various areas of chemistry and biology.[1] They are indeed involved in many chemical separation processes and they are also essential constituents of biological systems. Despite this importance, there have been relatively few spectroscopic investigations of the dynamics at liquid–liquid interfaces. The major reason is that the interfacial region represents a very small volume and therefore its contribution to the spectroscopic signal can, in principle, not be readily recovered because of the comparatively huge response from the bulk.

Several approaches can be used to circumvent this problem. The first one is to probe a material response that is specific to the interface. For example, second-harmonic generation occurs only at the interface between two liquids, where the centrosymmetry is broken.[2] The second approach is to probe a sample volume that comprises as less bulk material as possible. In this case, one can use an evanescent wave, generated by total internal reflection (TIR) at the interface, as the probe light.[3] The penetration depth of the evanescent light intensity is typically of the order of a quarter of wavelength, i.e., about 100–200 nm. If one compares this depth to the typical size of a molecule, one can wonder if the region probed by an evanescent wave is not already too large for the interfacial properties to be perceptible.

In order to answer this question, we have undertaken evanescent transient density phase grating measurements at liquid–liquid interfaces. As explained in more detail next, this technique allows the generation of a standing acoustic wave in the low refractive index medium. Its frequency is of the order of GHz and its wave vector is parallel to the interface. The propagation of this wave is detected optically with an evanescent probe pulse and its speed can be deduced. As the speed of sound in a material depends on its structure, which, in the case of a liquid, is expected to be modified at the interface, comparison of this value determined in the evanescent region with that obtained in the bulk solution will be a measure of the selectivity of the evanescent transient grating technique to the interface.

II. PRINCIPLE OF THE EVANESCENT TRANSIENT DENSITY PHASE GRATING TECHNIQUE

In a conventional transient density phase grating experiment,[4] the sample is excited by two crossed and time coincident pump pulses. Such an excitation leads to a spatial distribution of excited state population and, in most cases, of temperature and density. This results in a spatial modulation of the refractive index, a so-called density phase grating. If thermal expansion is impulsive, two counterpropagating acoustic waves are additionally generated. Because of their interference with propagation, the modulation amplitude of the density phase grating, Δn_d, exhibits a temporal oscillation:

$$\Delta n_d(t) = C[1 - \cos(\omega_{ac} t) \cdot \exp(-\alpha_{ac} v_{ac} t)], \tag{1}$$

where C is a constant that depends on material properties, α_{ac} is the acoustic attenuation constant, v_{ac} is the speed of sound, and ω_{ac} is the acoustic frequency, which is related to the crossing angle of the pump pulses, θ, at wavelength λ_{pu}:

$$\omega_{ac} = \frac{4\pi v_{ac} \sin(\theta/2)}{\lambda_{pu}}. \tag{2}$$

The density phase grating can be probed at different time delays after its formation by a third pulse at Bragg angle, θ_B. If the probe wavelength, λ_{pr}, is far from any absorption band of the sample, the diffracted intensity, I_{dif}, is related to the probe intensity, I_{pr} as:

$$\frac{I_{dif}}{I_{pr}} \cong \left(\frac{\pi d}{\lambda_{pr} \cos \theta_B} \right) \cdot \Delta n_d^2. \tag{3}$$

Because of the acoustic waves, the time profile of the diffracted intensity oscillates with a period $\tau_{ac} = 2\pi/\omega_{ac}$. The speed of sound in the material can be determined from this period and with Eq. (2).[5]

If the probe wavelength coincides with an absorption band, Eq. (3) no longer holds and the diffracted signal de-

a)Electronic mail: eric.vauthey@chiphy.unige.ch

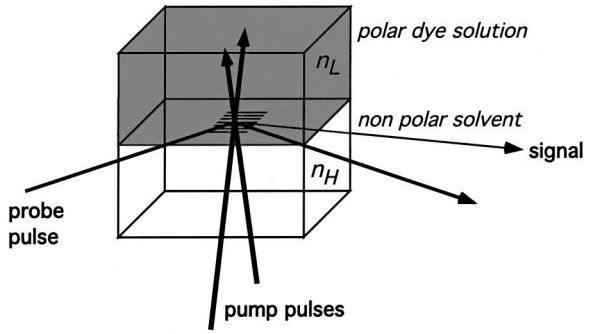

FIG. 1. Schematic of the evanescent transient grating setup.

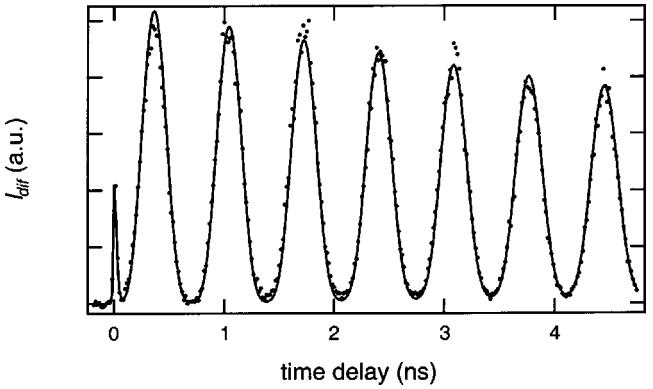

FIG. 2. Time profile of the diffracted intensity measured in the bulk with a solution of MG in MeOH and best fit of Eq. (3) with the additional contribution of population grating (solid line).

pends additionally on the squares of the absorbance change, ΔA_p, and of the Kramers–Kronig related refractive index change, Δn_p. If these changes decay faster than an acoustic period, the speed of sound can still be easily determined. Otherwise, interference effects between density and population gratings have to be considered.[6,7]

For the evanescent transient grating experiment, an ionic dye is dissolved in a polar low refractive index (n_L) solvent, which is in contact with a transparent, nonpolar, and high refractive index (n_H) liquid. The dye solution is excited by two pump pulses propagating through the transparent n_H medium and crossing at the interface. After absorption, nonradiative relaxation leads to the formation of a density phase grating in the n_L medium. As shown in Fig. 1, the probe pulse undergoes TIR at the interface. Its evanescent field interacts with the density phase grating and is partially diffracted. The evanescent signal appears in the n_H phase and its intensity is recorded.

Other beam configurations can be used: For example, the density phase grating can be generated upon interference between two crossed evanescent pump fields and probed with a pulse having an angle of incidence θ_B relatively to the normal of the interface.[8] The advantages and drawbacks of these two arrangements will be addressed next.

III. EXPERIMENT

A. Apparatus

The transient grating setup has been described in detail elsewhere.[9] In brief, the second-harmonic output pulses at 532 nm of a passive–active mode-locked Nd:YAG laser were split in three parts. Two parts were crossed in the sample cell (for bulk measurements) or at the interface, as shown in Fig. 1. The third pulse, the probe pulse, was first sent along a motorized optical delay line before striking the sample. For bulk measurements, the three pulses were arranged in a "boxcars" configuration. For measurements at the interface, the probe pulses were sent onto the interface with an angle of incidence that was varied between 70° and 80°, to undergo TIR. The pulse duration was around 25 ps and the total pump intensity on the sample was either of the order of 1 mJ/cm^2 (low intensity) or around 30 mJ/cm^2 (high intensity).

B. Samples

The absorbing dye was rhodamine 6G (R6G) at a concentration of 10^{-3}–10^{-2} M in methanol (MeOH) or acetonitrile (ACN), the n_L solvents. Decaline (DEC) was used as n_H solvent. About 20 ml of DEC were placed at the bottom of a $4\times4\times4$ cm^3 optical cell and about 5 ml of dye solution were added on top.

For bulk measurements, the absorbing dye was R6G (4×10^{-5} M) or malachite green (MG, 3×10^{-4} M) dissolved in the n_L solvents. The solutions were placed in a 1 mm thick optical cell.

IV. RESULTS

Figure 2 shows the time profile of the diffracted intensity measured in the bulk with a solution of MG in MeOH excited with two pulses crossed at 41.5°. The spike at time zero is the contribution of the population to the signal (ΔA_p and Δn_p), the ground-state recovery (GSR) of MG in MeOH occurring in a few ps. The continuous line is the best fit of Eqs. (1) and (3) with the additional contribution of the population. From such a signal, a speed of sound of 1104 m/s is found in MeOH, in excellent agreement with literature values.

The same measurement performed with 4×10^{-5} M R6G in MeOH results in a very different time profile. In this case, the signal is almost completely due to the contribution of the population and exhibits an exponential decay with a time constant of about 2 ns, half the GSR time of R6G. At high pump intensity, the time profile is similar to that measured with MG. This is due to biphotonic excitation, R6G(S_1) absorbing at 532 nm as well.[10] The ultrafast decay of the resulting upper excited state back to R6G(S_1) is accompanied by the release of about 2.4 eV as heat. High pump intensity also leads to a saturation of the population grating and therefore its contribution to the diffracted intensity is negligible. The speeds of sound obtained in these two experiments are essentially the same, within the limit of error.

Figure 3 shows the time profiles of the diffracted intensity measured with an evanescent probe pulse at the interface between DEC and R6G/MeOH, using low pump intensity and small crossing angle. As the amount of energy released as heat is small and as the acoustic period at this crossing

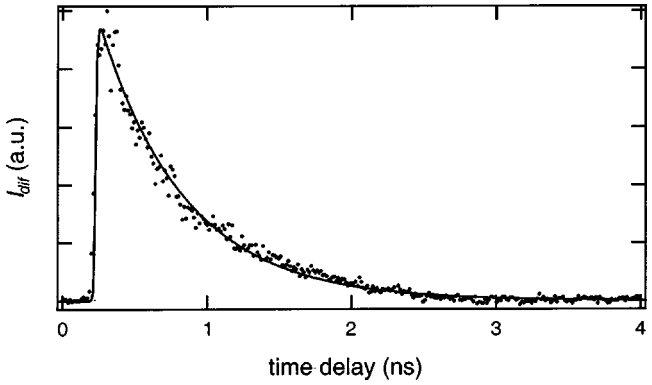

FIG. 3. Time profile of the diffracted intensity measured in the evanescent mode with a 10^{-2} M solution of R6G in MeOH in contact with DEC, using low pump intensity and small crossing angle. The solid line is the best fit of the theoretical expression assuming contribution of the population only.

angle is larger than 10 ns, the signal is due to population changes only. The GSR time of 1.2 ns calculated from this profile is smaller than that of about 4 ns obtained from the bulk experiment. This is due to the relatively high R6G concentration. Above 5×10^{-3} M, R6G form aggregates,[11] which shorten the S_1 lifetime of the monomer by energy transfer quenching. The ensuing excited aggregates decay nonradiatively with a time constant of the order of 1 ps.

Figure 4 shows the diffracted intensity measured with the same system but in ACN and with higher pump intensity and a crossing angle around 27°. The penetration depth of the probe pulse was 78 nm. The major difference between bulk and evanescent measurements is that the evanescent diffracted intensity exhibits a more complex oscillator pattern especially at small probe depth. In principle, such double oscillation can have two origins: Electrostriction[5] and destructive interference between the density phase grating (Δn_d) and a population phase grating (Δn_p).[7] However, the latter effect can be excluded first because Δn_p is negligibly small at 532 nm, which is close to the maximum of the absorption band of R6G, and second, because the first oscillation maximum does not appear at half the acoustic period, $\tau_{ac}/2$, as expected in this case. Indeed, the first clear oscillation maximum clearly appears later than $\tau_{ac}/2$ and a first maximum can be guessed as a shoulder before $\tau_{ac}/2$. This

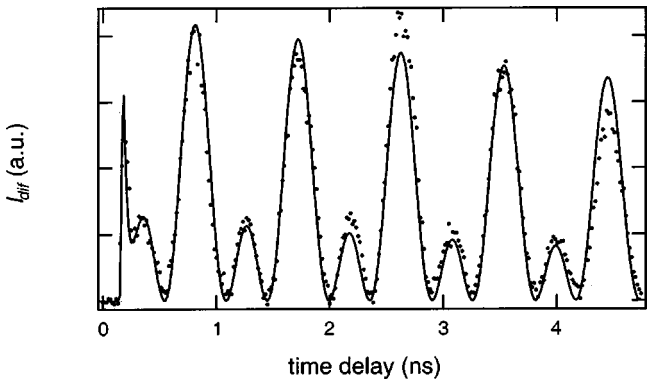

FIG. 4. Same as Fig. 3 but in ACN and with high pump intensity and large crossing angle (penetration depth: 78 nm). The solid line is the best fit of the theoretical expression assuming contributions of population, thermal expansion, and electrostriction.

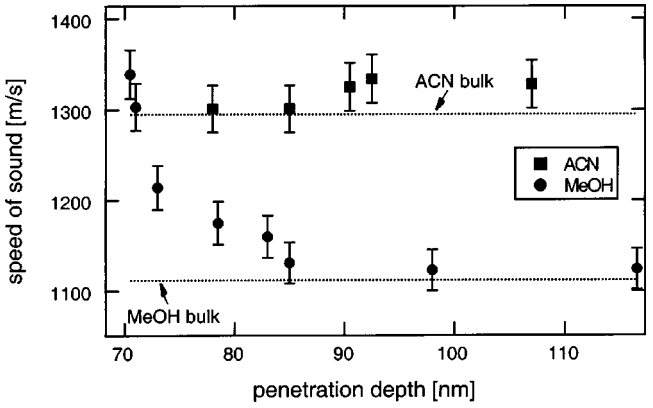

FIG. 5. Speed of sound as a function of the penetration depth in MeOH and ACN.

behavior can be reproduced by assuming that the acoustics are not only due to thermal expansion but also to electrostriction as shown by the solid lines in Fig. 4. As the probe depth increases, the relative contribution of electrostriction decreases in both solvents and vanishes above 110 nm.

The speeds of sound determined from the spacing between two oscillation maxima of the such time profiles measured at variable depths between 70 and 115 nm in MeOH and ACN are shown in Fig. 5. In ACN, there is no significant correlation between the speed of sound and the probing depth. The values are the same, within the experimental error, to that measured in the bulk.

The situation is different in MeOH, where the measured speed of sound increases systematically as the probing depth is decreased. At 115 nm, v_{ac} is close to the bulk value, while at 70 nm, it is apparently more than 20% larger!

V. DISCUSSION

The aforementioned results show clear differences between the evanescent and bulk time profiles, especially in MeOH. This is evidence that liquid–liquid interface properties can be discerned by evanescent probing. Our preliminary results indicate that the speed of sound in MeOH is considerably larger at the interface than in the bulk. As v_{ac} depends on the square root of the bulk modulus, this result can be interpreted as a higher rigidity of MeOH at the interface with DEC. It is well known that hydrophobic interaction at the interface favors a specific organization of the solvent molecules. This should occur with both MeOH and ACN. In MeOH however, this specific orientation can be somehow "locked" by hydrogen bonding, giving rise to a probably rather rigid structure. Moreover, due to hydrogen bonding, this specific structure may involve many more solvent layers than in ACN, where only dipole–dipole interaction is operative. Thus, the interface is presumably thicker with MeOH than with ACN. The interface with ACN is probably too thin relative to the evanescent probe depth to give rise to a significant difference in the speed of sound.

The relative contribution of electrostriction decreases markedly with increasing probe depth. This could be due to a higher third-order nonlinear susceptibility of the solvent at the interface.[12] However, effects related to the attenuation of

the optical field by the dye solution can not be totally excluded. In addition, the origin of this effect might also be due to a nonresonant contribution from the high refractive index solvent. Measurements to elucidate this are in progress.

Despite this, our results clearly show that transient grating with an evanescent probe is sensitive to the liquid–liquid interface, at least when the low refractive index solvent is protic. For the other solvents, the probe depth is probably still too large relative to the interfacial thickness.

As the diffracted intensity depends on the product of the intensity of the two pump and the probe pulses ($I_{dif} \propto I_{pu}^2 I_{pr}$), two variants of the technique used here can be envisaged to further improve the selectivity to the interface:

(1) evanescent pumping/normal probing: the penetration depth is decreased by a factor of 2. In this geometry, either the probe or the signal pulse has to cross the dye solution. Therefore, the probe wavelength must be out of the absorption spectrum of the dye; and
(2) evanescent pumping/evanescent probing: the penetration depth is decreased by a factor of 3, and can thus be as small as 20 nm. Moreover, the absorption of the probe or signal pulse is no longer a problem.

The implementation of these variants is in progress.

In conclusion, the evanescent transient grating techniques offer a promising perspective for investigating dynamic processes at interfaces.

ACKNOWLEDGMENTS

This work was supported by the Fonds National Suisse de la Recherche Scientifique through project 2000-0632528.00.

[1] *Liquid–Liquid Interfaces*, edited by A. G. Volkov and D. W. Deamer (Chemical Rubber Corp., Boca Raton, FL, 1996).
[2] K. B. Eisenthal, Chem. Rev. **96**, 1343 (1996).
[3] S. Ishizaka and N. Kitamura, Bull. Chem. Soc. Jpn. **74**, 1983 (2001).
[4] M. Terazima, Adv. Photochem. **24**, 255 (1998).
[5] R. J. D. Miller, R. Casalegno, K. A. Nelson, and M. D. Fayer, Chem. Phys. **72**, 371 (1982).
[6] K. A. Nelson, R. Casalegno, R. J. D. Miller, and M. D. Fayer, J. Chem. Phys. **77**, 1144 (1982).
[7] E. Vauthey and A. Henseler, J. Phys. Chem. **99**, 8652 (1995).
[8] N. Tamai, T. Asahi, and T. Ito, in *Microchemistry, Spectroscopy and Chemistry in Small Domains*, edited by H. Masuhara, F. C. De Schryver, N. Kitamura, and N. Tamai (Elsevier Science, Amsterdam, 1994), p. 241.
[9] C. Högemann, M. Pauchard, and E. Vauthey, Rev. Sci. Instrum. **67**, 3449 (1996).
[10] J.-C. Gumy and E. Vauthey, J. Phys. Chem. **100**, 8628 (1996).
[11] A. Penzkofer and Y. Lu, Chem. Phys. **103**, 399 (1986).
[12] T. Tsang, Phys. Rev. A **54**, 5454 (1996).